Carbohydrate Polymers 80 (2010) 35–43

Contents lists available at ScienceDirect

Carbohydrate Polymers

journal homepage: www.elsevier.com/locate/carbpol

Characterization of microcrystalline cellulose and cellulose long fiber modified by iron salt

Smith T. Sundar [a,*], Mohini M. Sain [a], Kristiina Oksman [a,b]

[a] Centre for Biocomposites and Biomaterials Processing, Faculty of Forestry, University of Toronto, 33 Willcocks St., Toronto, Ont., Canada M5S3B3
[b] Manufacturing and Design of Wood and Bionanocomposites, Luleå University of Technology, SE-971 87 Luleå, Sweden

ARTICLE INFO

Article history:
Received 10 July 2009
Received in revised form 20 October 2009
Accepted 28 October 2009
Available online 3 November 2009

Keywords:
Cellulose complexes
Cellulose long fiber
Iron complex
Microcrystalline cellulose

ABSTRACT

Microcrystalline cellulose (MCC) and cellulose long fiber (CLF) were treated with iron (Fe) based salt and the samples were characterized to study the coordination complexes formed between cellulose and iron. The Fe-modified MCC and CLF were characterized by spectroscopic, thermal and morphological methods. MCC and CLF were oxidized and further treated with iron (Fe) based salt in a high pH medium to form coordination complexes. Both MCC and CLF were then analyzed using Scanning electron microscopy (SEM) to examine their surface morphology. The results have shown that there was no major change in morphology for MCC and CLF upon modification. The functional groups formed by modifying cellulose by iron salt were investigated using FTIR-ATR spectroscopy and the nature of the coordination bonds formed between cellulose and Fe ions were examined by X-ray photo electron spectroscopy (XPS). The results agree that coordination bonds were formed between de-protonated and or oxidized hydroxyl group and Fe ions. Powder XRD (PXRD) was resourceful to compare the crystallinity of unmodified and Fe-modified samples of MCC and CLF. Thermal stability of modified cellulose was studied using thermo gravimetric analysis (TGA). The results showed that there was an increase in percentage of residual mass and higher thermal stability for the Fe-modified MCC and CLF compared to unmodified samples due to the presence of iron.

1. Introduction

Cellulose is one of the most abundant naturally occurring biopolymer. It is commonly found in the cell walls of plants and certain algae. In addition to plant cell wall, cellulose can be obtained from sources like tunicates (Angles & Dufresne, 2000; Sturcova, Davies, et al., 2005) and bacteria (Bielecki & Krystynowicz, 2002).

Cellulose from the bacterium *Acetobactor xylinum* is a product of its primary metabolism and forms a protective coating in contrast to the structural roles cellulose plays in plant cell wall (Bielecki & Krystynowicz, 2002). Recently, there has been a great deal of research interest in utilizing cellulose for various applications such as composite manufacturing due to its remarkable reinforcing capability, excellent mechanical properties, low density and environmental benefits. However, the reinforcing capability of cellulose can be compromised by the poor dispersion and lack of orientation of cellulose fiber in the polymer matrix (Larenjeria, Carvalho, Silva, & D'Almedia, 2006). Recent studies have shown that orientation of cellulose can be achieved by subjecting the cellulose fiber suspended in a solution to electromagnetic fields. Liquid suspension of cellulose when dried in an electric field was oriented in respect to the applied electric field (Bordel, Putaux, & Heux, 2006). Orientation of cellulose fibers in suspensions were reported when they were subjected to magnetic fields up to 20 T (Cranston & Gray, 2006; Kvien & Oksman, 2007; Sugiyama, Chanzy, & Maret, 1992). In this scenario, it justifiable to modify cellulose with paramagnetic elements such as iron to induce further improvement in cellulose orientation in a polymer matrix. Such modification could enhance orientation of cellulose in lower strength electric and magnetic fields.

Cellulose has been modified to obtain various derivatives such as acetates and nitrates. Among the derivatives, cellulose-based metal complexes have attracted scientists due to its specific applications. Cellulose–metal complexes have found many foreseeable applications in drug delivery systems and initiators for free radical polymerization (Harcourt, 1972; Muller, Hebert, & Rollins, 1971; Samal, Satrusallya, & Sahoo, 1984). However, to the best of our knowledge, there is only little information available regarding the synthetic routes used to produce these cellulose-metal complexes. When transition metal salts are reacted with cellulose, they form coordination bonds with functional groups at the 6th, 2nd and 3rd carbon positions of cellulose. Previous studies have revealed that it is possible to form coordination bonds involving transition metals and monosaccharides such as glucose, fructose and galactose (Cerchiaro, Carlos, Laudelina, Temperini, & Ferreira,

* Corresponding author. Tel.: +1 416 946 3191; fax: +1 416 978 3834.
E-mail address: smith.sundar@utoronto.ca (S.T. Sundar).

0144-8617/$ - see front matter © 2009 Elsevier Ltd. All rights reserved.
doi:10.1016/j.carbpol.2009.10.072

2005). There have been studies on derivatives of cellulose such as hydroxyethyl cellulose (HEC) and carboxymethyl cellulose (CMC), when reacted with iron salts have produced cellulose–Fe coordination complexes (El-Saied, Basta, Abdel-hadi, & Hosny, 1994). Transition metals will complex with de-protonated hydroxyl group of polysaccharides through oxo-bridges (Hosny, Basta, & El-Saied, 1997). Cellulose, a polysaccharide having β (1–4)-linked glucopyranose units, the vicinal diol groups (2- and 3-hydroxyl groups) can be involved in the formation of diketone bonds in coordination with Fe^{2+} (Godovsky et al., 1999). However, the primary hydroxyl groups of cellulose at C6 have the potential to form complexes with adjacent cellulose chain through Fe bridges (Fig. 5). The hydroxyl groups at C6 may not form Fe complexes with C2 and C3 of the same cellulose molecule owing to their steric hinderance (Kennedy, Barker, & Zamir, 1974). The specific objective of this study is to characterize the coordination bonds formed between Fe and modified hydroxyl groups. The functional groups formed upon modification, the nature of bonds, surface morphology and thermal properties of MCC and CLF was also investigated using FTIR, XPS, SEM and TGA, respectively.

2. Experimental

2.1. Materials

MCC (Avicel, PH-101) was purchased from Fluka, Biochemika and CLF was purchased from Sigma–Aldrich, Canada. Both MCC and CLF were used as obtained without any further processing. Ferrous sulfate $FeSO_4{\cdot}7H_20$ (98% purity) obtained from Fluka Chemika and Hydrogen peroxide 30% v/v was used.

2.2. Oxidation

The dissociation of hydrogen peroxide at high pH results in formation of perhydroxyl anions which acts as an oxidizing agent (Zeronian & Inglesby, 1995). Such an oxidation can modify cellulose hydroxyl groups into oxycellulose. The hydroxyl groups can also get modified into carboxylic and or keto groups (Lewin & Ettinger, 1969).

Twenty-five grams of MCC and CLF were soaked separately in 1 M NaOH and stirred at room temperature for 50 h to aid intracrystalline swelling. 250 mL of hydrogen peroxide (30% v/v) was added to 1000 mL of alkaline cellulose suspension and stirred for 15 h in room temperature (25 ± 1 °C) and pressure (Zeronian & Inglesby, 1995). The suspension was washed with distilled water three times and further vacuum filtered to obtain the fiber and used as such for further reaction with iron salts.

2.3. Preparation of cellulose–Fe complexes

The formation of cellulose–Fe bonds are based on *in situ* coordination bonds between Fe and its intermediate ions with modified 2, 3 and 6 hydroxyl groups in cellulose. Cellulose–metal complexes were prepared by reacting oxidized cellulose with ferrous sulphate hepta hydride ($FeSO_4{\cdot}7H_2O$). $FeSO_4{\cdot}7H_2O$ which was pre-treated with NaOH to liberate Fe^{2+} ions. The oxidation state of Fe in the presence of NaOH are depended on pH and the concentration of Fe^{2+} ions (Godovsky et al., 1999). At $R = 7/12$ (R = ratio between $FeSO_4$ and NaOH) the proposed reaction produces Fe^{2+} ions available to form complexes with modified hydroxyl groups of cellulose (Olowe, Marie, Refait, & Genin, 1994).

$$7FeSO_4 + 12NaOH \rightarrow 6Fe(OH)_2 + 6Na_2SO_4 + Fe^{2+} + SO_4^{2-}$$

Oxidized cellulose (MCC and CLF) were added to two separate solutions of NaOH (1 M) with 16.6 g of $FeSO_4{\cdot}7H_2O$. The mixture was stirred for 7 h at room temperature (25 ± 2 °C). Then the reaction mixture containing cellulose fiber was filtered and washed several times in double distilled water until the pH became neutral. The reaction products were dried in an oven at 50 °C for 48 h and stored in an air tight container for further analysis.

2.4. Scanning electron microscopy (SEM)

Morphology of the fibers after treatment was analyzed with an SEM. The analysis was carried out using a Hitachi S-2500 scanning electron microscope. The samples were mounted on metal stubs using double side adhesive tapes. Scanning electron micrographs of dried MCC and CLF samples (both control and treated) were obtained at an acceleration voltage of 15 kV. The samples were previously sputter coated with gold for 30 s using a Cresingtor plasma sputter coater.

2.5. Fourier transform infrared spectroscopy (FTIR)

FTIR analysis was conducted to study the functional groups present in MCC and CLF before and after chemical modification with iron salts. FTIR experiments were performed using a Bruker Tensor 27 instrument. An attenuated total reflectance (ATR) mode was engaged to obtain information on the surface functionalities of the cellulose fibers. The instrument was operated at 4 cm^{-1} resolution and samples were subjected to 45 scans/s. The spectra was recorded in an absorbance mode and thoroughly analyzed for all absorption peaks from wavenumbers 4000 to 400 cm^{-1}.

2.6. X-ray photoelectron spectroscopy (XPS)

XPS spectra were obtained by running the cellulose samples on a Thermo Scientific with a monochromatic Al-Kα X-ray source. The spot size used for analysis was approximately 400 μm. A charge compensation was provided and position of the energy scale was adjusted to place the main cellulosic C1s feature (C—O) at 286.5 eV. Samples were analyzed at a take off angle of 90° with respect to the surface.

A low resolution survey spectrum ranging from 0 to 1350 eV was obtained to survey the elements present in the sample. The spectra collected at low resolution mode for survey was at 150 eV pass energy. To characterize the relative atomic percentage, a high-resolution spectrum ranging from 280 to 300 eV, 524 to 538 eV and 700 to 750 eV binding energy was obtained for the C1s, O1s and Fe2p regions respectively. High resolution mode used 20 eV as pass energy to scan C, O and Fe regions. The bond analysis of was determined by curve fitting the peaks for C1s, and Fe2p and deconvoluting the peaks into sub-peaks. The data was analyzed using Avantage onboard software supplied by Thermo Scientific with the instrument. The atomic ratio of oxygen to carbon (O/C) was calculated from corresponding peak area based on the equation

$$O/C = [I_O/I_C] \times (S_C/S_O)$$

where I_O and I_C are the integrated peak area for oxygen and carbon, respectively. S_C/S_O is corrected sensitivity factor.

2.7. Powder X-ray diffraction (PXRD)

The powder X-ray diffraction (PXRD) patterns of treated and untreated MCC and CLF were recorded using a Rigaku–Panalytical diffractometer which produce CuK-α emission lines. A nickel filter was used to eliminate K-β X-rays. The diffractometer was operated at 40 kV at 40 mA in the range of 5–45°.

2.8. Thermal analysis

Thermal degradation characteristics of Fe-modified and unmodified MCC and CLF were analyzed using a TGA Q 500 series thermogravimetric analyzer. The ramping rate was 10 °C/min up to 700 °C in a nitrogen environment. The results were reported in % weight loss versus temperature. The percentage of residual mass before and after modification of MCC and CLF were compared to establish iron content present in Fe-modified samples.

3. Results and discussion

Fe-modified and control samples of MCC and CLF were characterized using SEM to understand its surface morphology. Five replicates from three different samples were analyzed and a wide range of distribution in the aspect ratio (length/breadth) was observed for both MCC and CLF. The length of MCC ranged from 10 to 100 μm and the diameter ranged from 5 to 10 μm. The aspect ratio for MCC was in the range of 3.0–7.5. In Fig. 1 the visual inspection of these images indicated that there is no considerable morphological changes occurred on the MCC surface due to the treatment. The CLF, analyzed using SEM ranged from 70 to 350 μm in length and 5 to 15 μm in breadth. The aspect ratio for CLF was in the range of 10.0–21.0. A comparison between SEM images of treated and untreated CLF showed that the cellulose fibers less than 20 μm in length are absent in the Fe-modified samples. These particles could very well be lost during washing the samples in order to bring the samples to neutral pH. Fig. 2 showed slight stranding of fiber at the ends on CLF surface after NaOH treatment. The intercrystalline swelling by NaOH and stirring of cellulose might have resulted in damaging the ends of CLF fibers.

Pure, oxidized and Fe-modified MCC and CLF were examined by FTIR in ATR (attenuated total reflectance) mode. The spectra for MCC are shown in Fig. 3. After oxidation of MCC peaks corresponding to carbonyl groups were observed at 1731.63 cm^{-1}. The peaks of interest for Fe-modified MCC samples were at 3838 cm^{-1}, 3742 cm^{-1}, 1516 cm^{-1} and 490 cm^{-1}. For oxidized CLF shown in Fig. 4, the peaks of interest were at 1693.03 cm^{-1} related to carbonyl groups. For Fe-modified CLF, peaks were observed at 3841 cm^{-1}, 3743 cm^{-1}, 1517 cm^{-1} and 498 cm^{-1}. The intense bands in the region of 4000–3000 cm^{-1} are attributed to free hydroxyl and bonded OH stretching vibrations (Coates, 2000). In the case of both Fe-modified MCC and CLF there were additional shoulders in this region. The two shoulder peaks formed in the region of 4000–3740 cm^{-1} are assigned to the cleavage of the primary and secondary hydroxyl groups involved in the coordination complex formation with Fe (Hosny

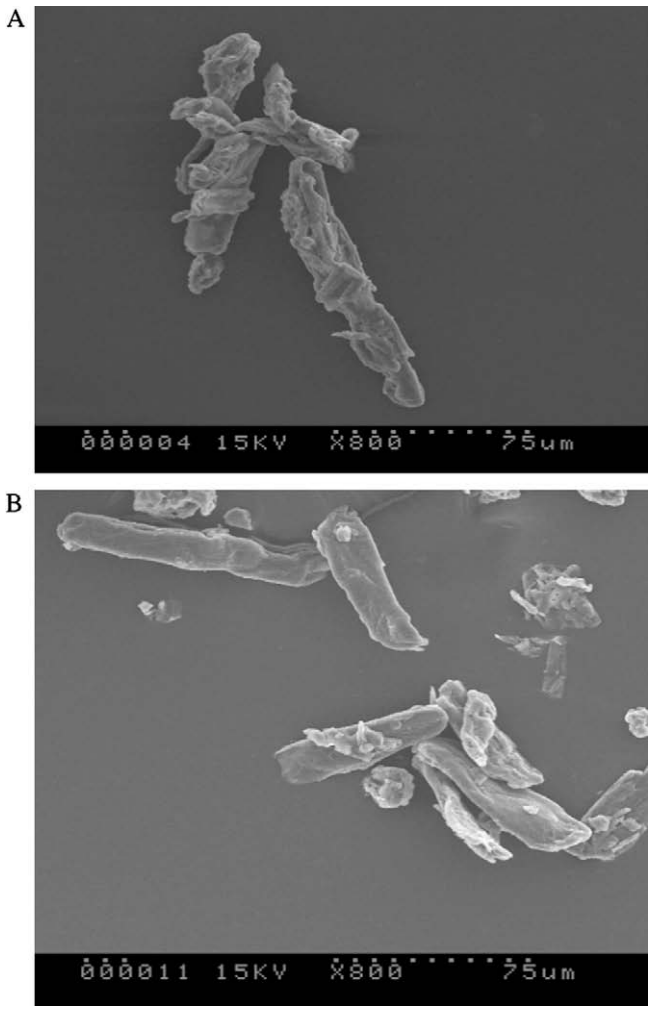

Fig. 1. Scanning electron micrographs of (A) unmodified and (B) modified microcrystalline cellulose (MCC).

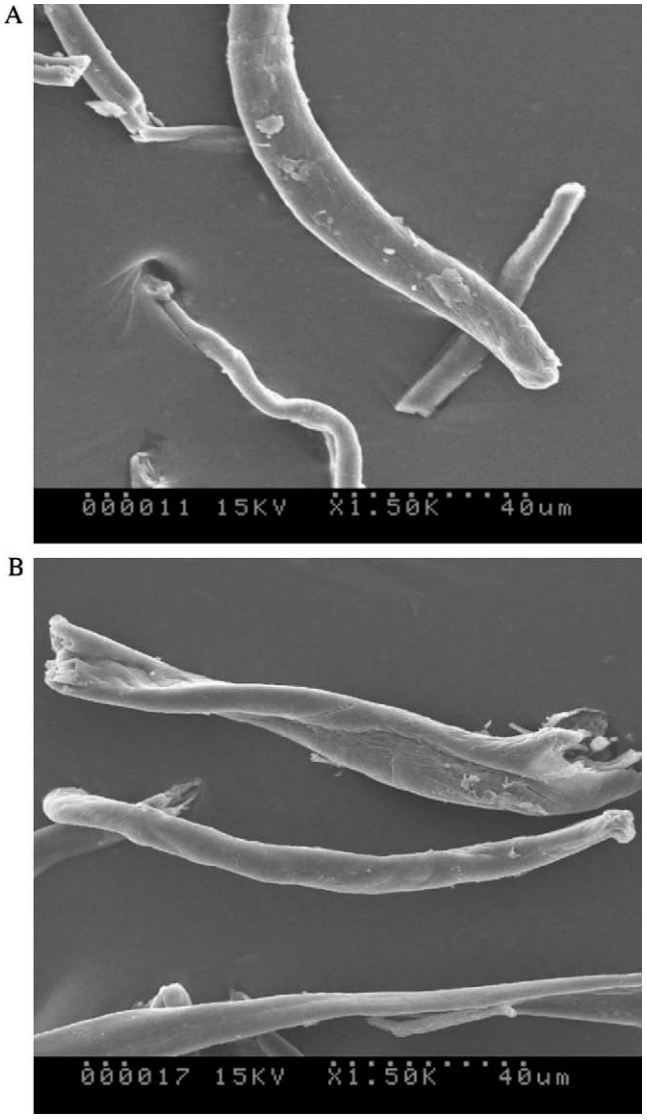

Fig. 2. Scanning electron micrographs of (A) unmodified and (B) modified cellulose long fiber (CLF).

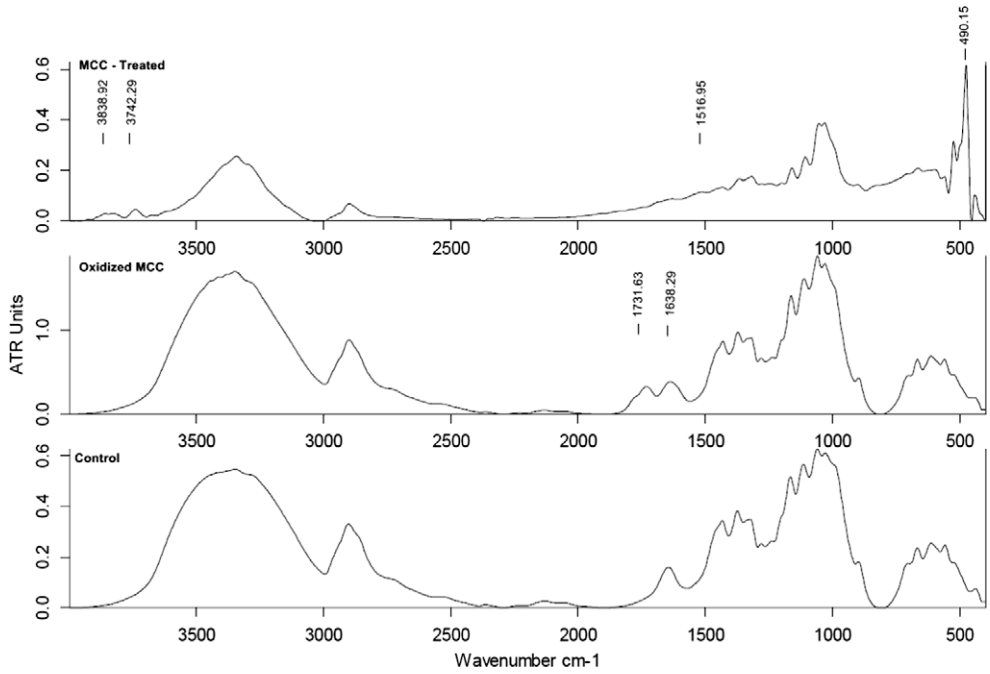

Fig. 3. FTIR spectra of MCC control, oxidized MCC and treated MCC.

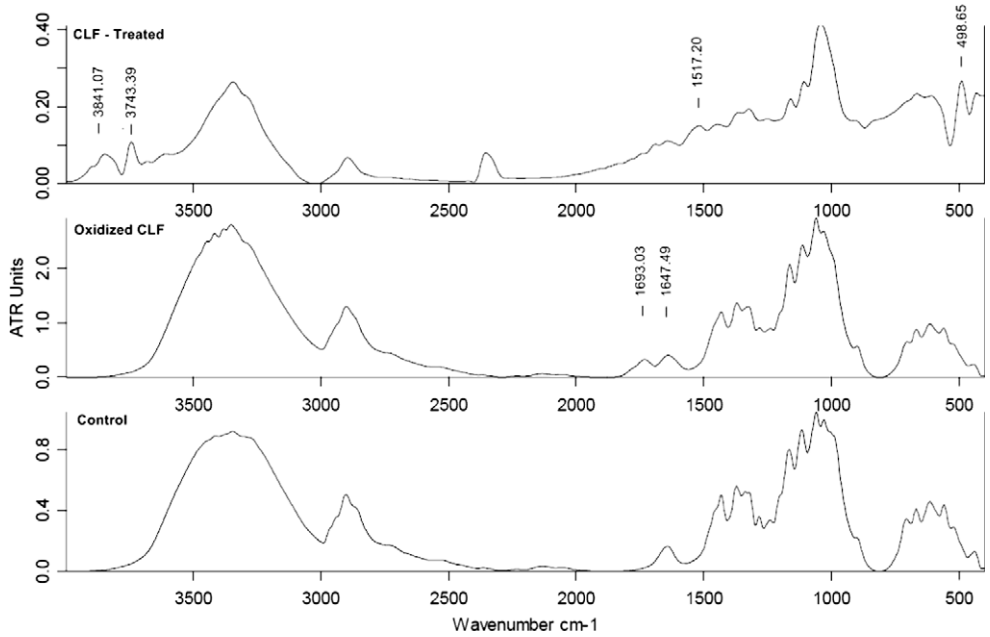

Fig. 4. FTIR spectra of CLF-control, oxidized CLF and treated CLF.

et al., 1997). The strong peak from 3500 to 3000 cm^{-1} shows presence of unreacted hydroxyl groups in both MCC and CLF (Coates, 2000). The weak peaks from 1510 to 1520 cm^{-1} are characteristic to diketone and its metal–oxygen derivatives formed by coordination with Fe^{2+} ions resulting in diketone/quinone metal complexes (Wijnja & Schulthess, 2001). The Fe^{2+} ions are bonded to 2nd and 3rd hydroxyl groups of cellulose that have been oxidized to keto groups and or carboxylate groups upon treatment with hydrogen peroxide. The peak in this region (1510–1520 cm^{-1}) represents the asymmetrical vibration of O═C—C═O or bi dentate Fe^{2+} complex such as —C—O—Fe—O—C— engaged in coordinate bond formation (Bock, Karsten, Helmut, Kuhr, & Musso, 1971) (Fig. 5). The peaks observed around 490–510 cm^{-1} for both Fe-modified MCC and CLF are essentially from vibration of metal oxide bonds. These bonds are believed to be from de-protonated hydroxyl groups of modified cellulose and Fe^{2+} ions (Offiong, 1995).

X-ray photo electron spectroscopy analysis was performed to determine the presence of elements in the unmodified and Fe-modified cellulose samples. In Figs. 6A and 7A, a low resolution scan mode has shown that the primary elements present in the unmodified MCC and CLF were mainly C and O. A low resolution scan for pure $FeSO_4{\cdot}7H_2O$ was also obtained for elemental analysis. Peaks were obtained for C, O, S and Fe (Fig. 8). The presence of iron was distinctive in the low resolution scan of Fe-modified cellulose

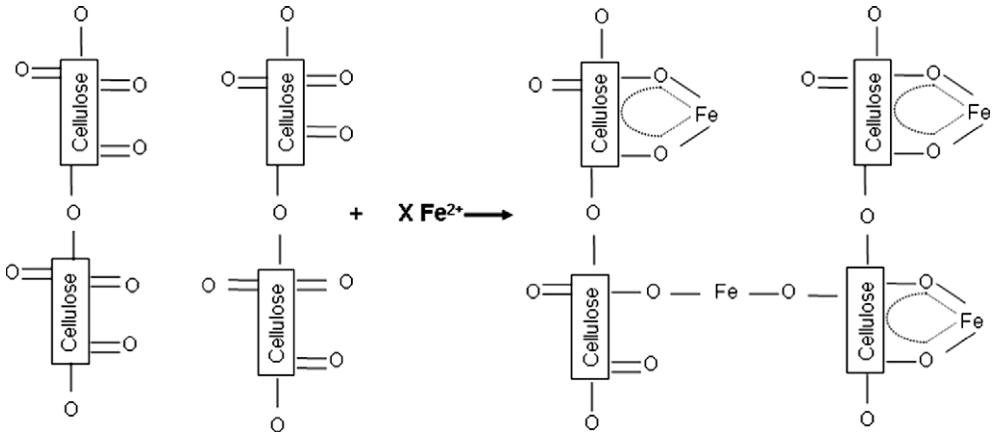

Fig. 5. Schematic of proposed complexation of iron with cellulose.

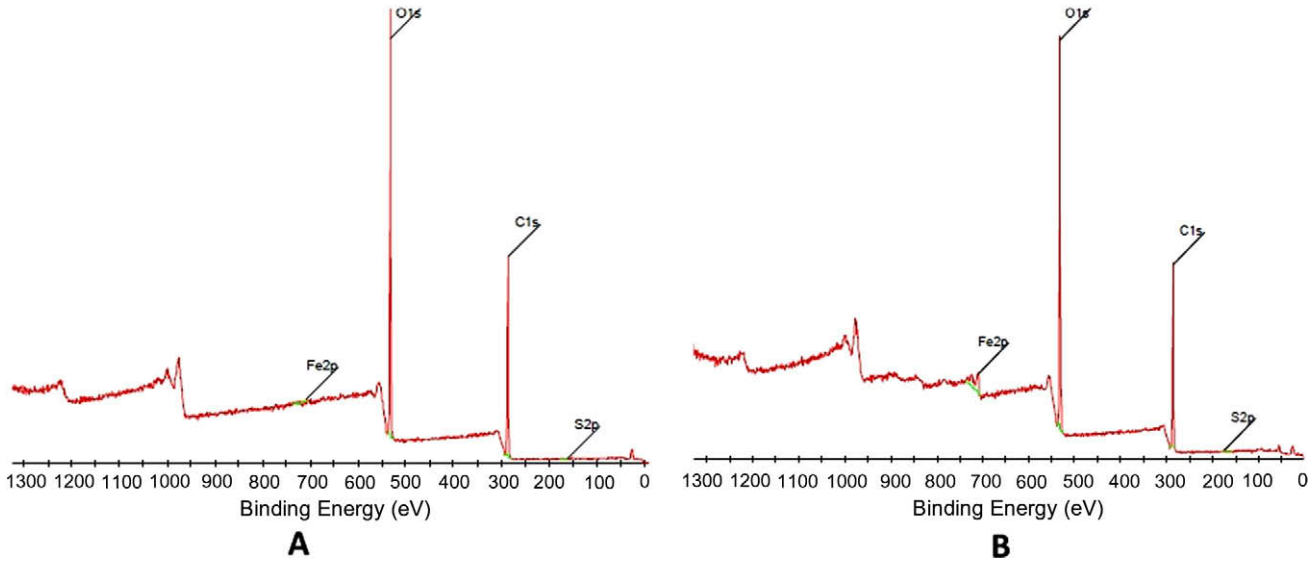

Fig. 6. XPS survey spectrum for untreated (A) and treated (B) MCC.

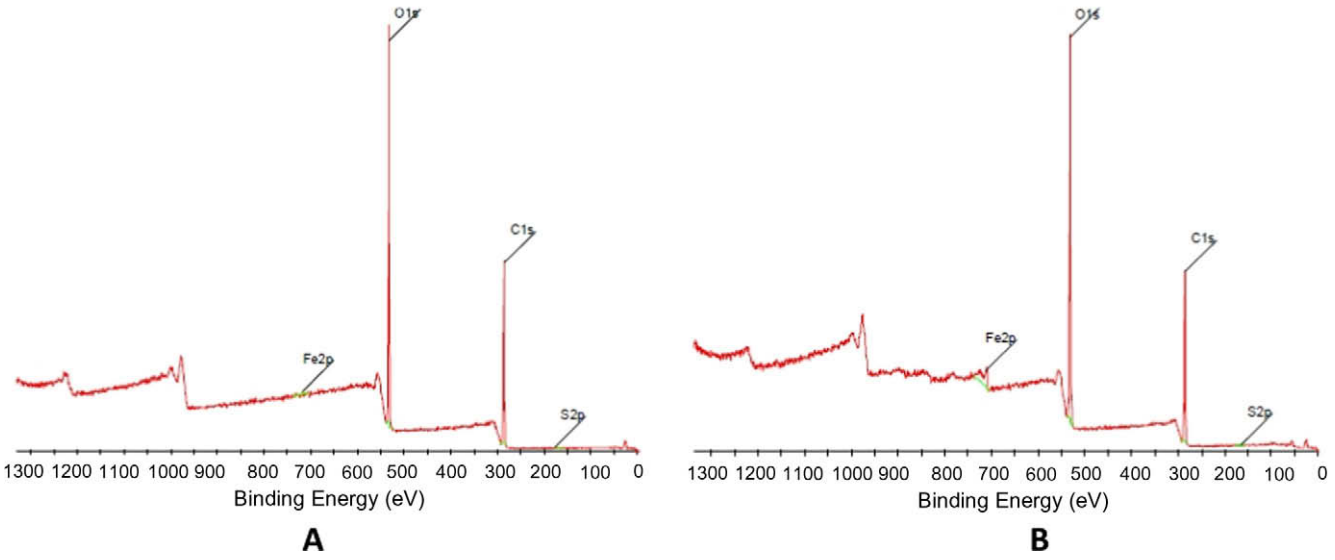

Fig. 7. XPS survey spectrum for untreated (A) and treated (B) CLF.

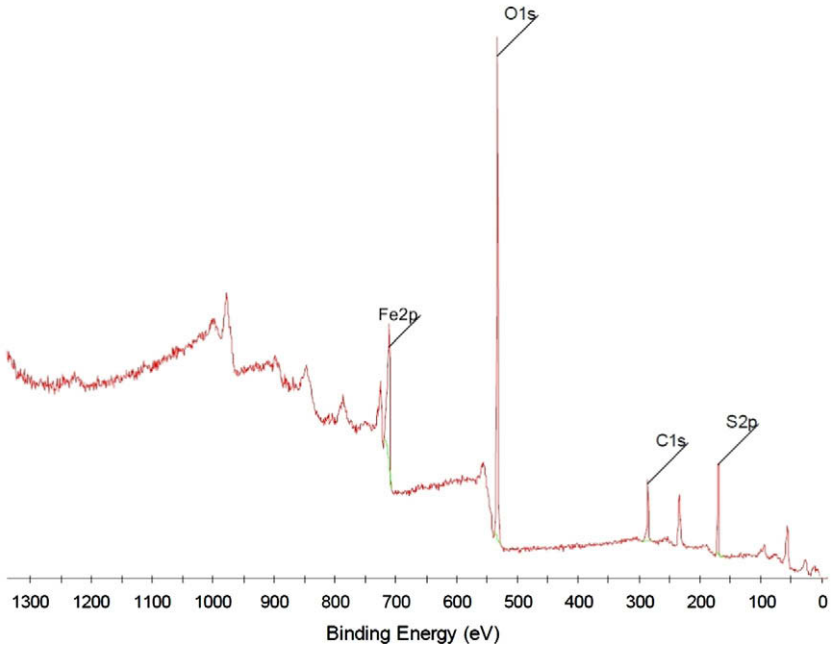

Fig. 8. XPS survey spectrum for ferrous sulphate hepta hydrate.

samples (Figs. 6B and 7B). A high resolution scan was completed on the C1s and Fe2p region of Fe-modified MCC and CLF. The oxygen/carbon [O/C] ratio was calculated to determine the surface oxidation of the samples after modification (Allen, Curtis, Hooper, & Tucker, 1974). The oxygen to carbon ratio for Fe-modified MCC and CLF was higher than that of the unmodified samples suggesting the oxidation of hydroxyl groups (Table 1). The modification of hydroxyl groups to ketones and carboxylates resulted in addition of oxygen atoms resulting in higher O/C ratio in Fe-modified cellulose.

A high resolution scan of the C1s region of Fe-modified and unmodified MCC and CLF was deconvoluted into three sub-peaks namely C1s-HR-A, C1s-HR-B and C1s-HR-C. The deconvoluted peaks of C1s region and their corresponding binding energy and bond type are shown in Table 2. The C1s peak at 284.87 eV corresponds to carbon hydrogen bonds while C1s-HR-A, C1s-HR-B and C1s-HR-C correspond to various carbon–oxygen bonds. These peaks have arised from basic structure of cellulose where carbon atoms are attached to hydrogen and from unreacted ketone and carboxyl groups and possibly from the cyclic hemi-acetal linkage structure in cellulose chain (Hon, 1984).

The presence of peaks in the region of 700–730 eV showed the occurrence of coordination bonds of Fe with Oxygen in both Fe-modified MCC and CLF. Table 1 shows that the percentage of iron present in the modified samples was 1.95% and 1.85% for MCC and CLF respectively. The peak binding energy for Fe2p curves for Fe-modified MCC was 710.39 eV and for CLF it was 710.51 eV (Tables 3 and 4). Representative images for deconvoluted Fe2p peaks are shown in Figs. 9 and 10 for MCC and CLF, respectively. The high resolution peaks of interest in this region were Fe2p-HR-A and Fe2p-HR-B. The binding energy for Fe2p-HR-A and Fe2p-HR-B for modified MCC and CLF and their corresponding bond types were obtained from the data base for XPS spectral lines from National institute of standards and technology (NIST), USA. The numerical values for the resolved peaks, values for theoretical binding energy and corresponding bond type are represented in Tables 3 and 4. The data shows that both Fe2p-A and Fe2p-B peaks in MCC and CLF are based on iron–oxygen bonds (Bock et al., 1971; Cerchiaro et al., 2005). Oxygen atoms bonded to iron are essentially from the de-protonated and or oxidized hydroxyl groups of cellulose (Hegetschweiler et al., 1995; Skopenko et al., 2004). High pH and the presence of an oxidizing agent such as hydrogen peroxide oxidize the hydroxyl group of cellulose into ketones or carboxylates. When Fe^{2+} ions were introduced to modified cellulose functional groups has resulted in the formation of Fe-oxo bridged polyolato complexes (Hegetschweiler et al., 1995; Spikes, Bill, Weyhermuller, & Wieghardt, 2008). Fe-oxo bridged complexes were speculated to be aroused from the coordination between diketones with iron and from de-protonated hydroxyl groups of cellulose and iron. The FTIR peaks obtained at 490–510 cm^{-1} due to formation of metal–oxide bonds holds good with the result from XPS peaks of Fe–oxygen ranging from 700 to 730 eV. XPS was further helpful to identify the nature of bonds formed between oxidized and or de-protonated cellulose and iron. A high-resolution spectrum for the Fe region of $FeSO_4{\cdot}7H_2O$ was also obtained to compare it with the peaks obtained from Fe region of modified MCC and CLF. The peak binding energy for Fe2p region was 711.11 eV corresponding to pure $FeSO_4{\cdot}7H_2O$. It should also be noted that in Fe-modified MCC and CLF, the peak for Sulpher was absent confirming the absence of residual $FeSO_4{\cdot}7H_2O$.

Crystalline peaks of MCC and CLF were recorded using a Powder X-ray diffractometer. The PXRD pattern for both Fe-modified and unmodified MCC exhibit diffraction peaks at 16.2θ and 22.18θ which represents crystalline structure of cellulose 1 (Fig. 11) (Nelson, 1964). Sharper PXRD peaks corresponded to higher crystallinity of the sample. However the intensity of the peak for Fe-modified MCC was lesser compared to unmodified samples. The

Table 1
Elemental analysis of modified and unmodified MCC and CLF using a low resolution XPS spectrum.

Samples	Elemental composition (%)			O/C
	C	O	Fe	
MCC	57.86	42.14	0.00	0.63
MCC treated	54.35	43.7	1.95	0.70
CLF	58.98	41.02	0.00	0.60
CLF treated	54.69	43.46	1.85	0.68

Table 2
Analysis of C1s peak from XPS spectra.

Sample	C1s [C—C]		C1s-HR-A [C—O]		C1s-HR-B [C=O]		C1s-HR-C [O—C=O]	
	eV	%	eV	%	eV	%	eV	%
MCC	284.87	11.21	286.52	63.81	287.87	23.27	289.52	1.70
MCC (T)	284.87	14.85	286.44	60.77	287.85	22.73	289.66	1.66
CLF	284.90	15.41	286.50	59.85	287.85	22.85	289.50	1.89
CLF (T)	284.88	13.57	286.44	60.14	287.83	24.42	289.60	1.87

Table 3
(MCC) Deconvoluted peaks of Fe2p region of modified MCC–Fe complex and corresponding bond type.

Peak	Binding energy (BE)	At.%	Bond type
Fe2p	710.39	24.76	Fe or Fe—O—
Fe2pA	709.55	36.37	Fe—O—
Fe2pB	711.50	14.70	Fe—[OH]—O

Table 4
Deconvoluted peaks of Fe2p region of modified CLF–Fe complex and corresponding bond type.

Peak	Binding energy (BE)	At.%	Bond type
Fe2p	710.51	26.45	Fe or Fe—O—
Fe2pA	709.68	34.88	Fe—O—
Fe2 B	711.46	16.45	Fe—[OH]—O

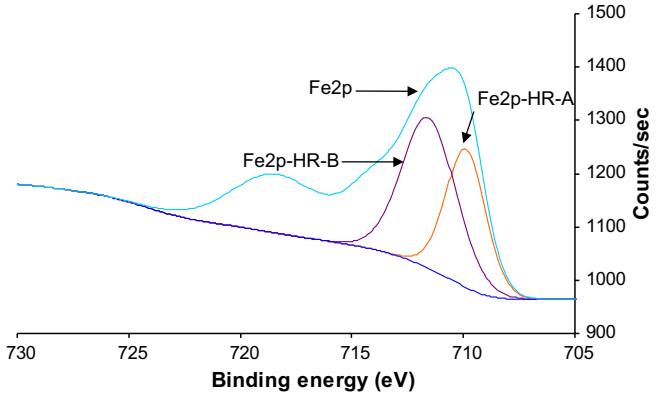

Fig. 9. High resolution XPS peak of Fe2p region of modified MCC.

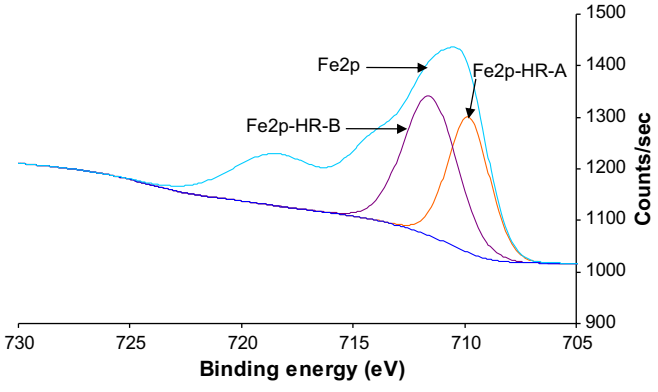

Fig. 10. High resolution XPS peak of Fe2p region of modified CLF.

lower peak intensity of modified MCC might have aroused due to treatment with NaOH (Nelson & L, 1964; Oh & et al., 2005). The

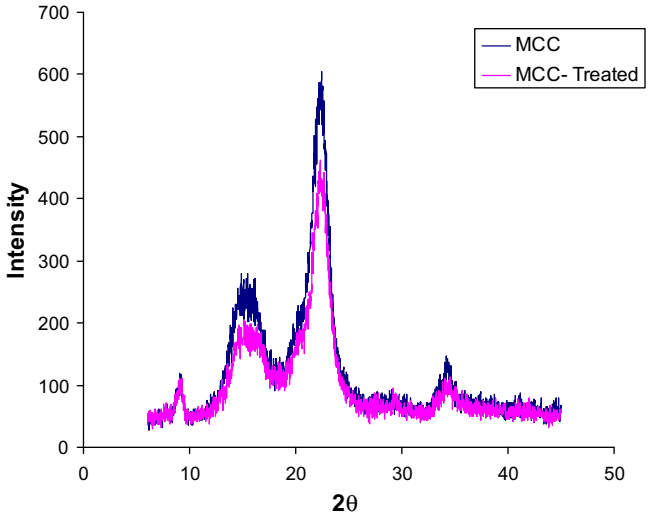

Fig. 11. PXRD patterns of untreated and treated MCC.

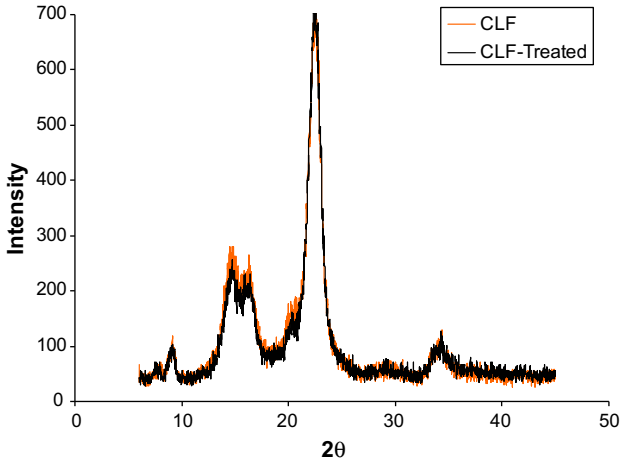

Fig. 12. PXRD patterns of untreated and treated CLF.

crystalline region of MCC could have dismantled due to treatment with NaOH. Fig. 12 showed that for both Fe-modified and unmodified CLF, the peaks at 14.5 and 16.3 were wide, a sharp peak was observed at 22.58 representing crystalline region of CLF. There were no comparable differences in peak intensity for both CLF samples.

Thermal characterization of MCC and CLF can give insight into the processability of the fibers when mixed with a polymer. The thermograph results for both Fe-modified and unmodified MCC and CLF shows that there was a weight loss at 100–105°C due to evaporation of moisture. For untreated MCC the degradation occurred at a temperature range of 304–348 °C. The results from

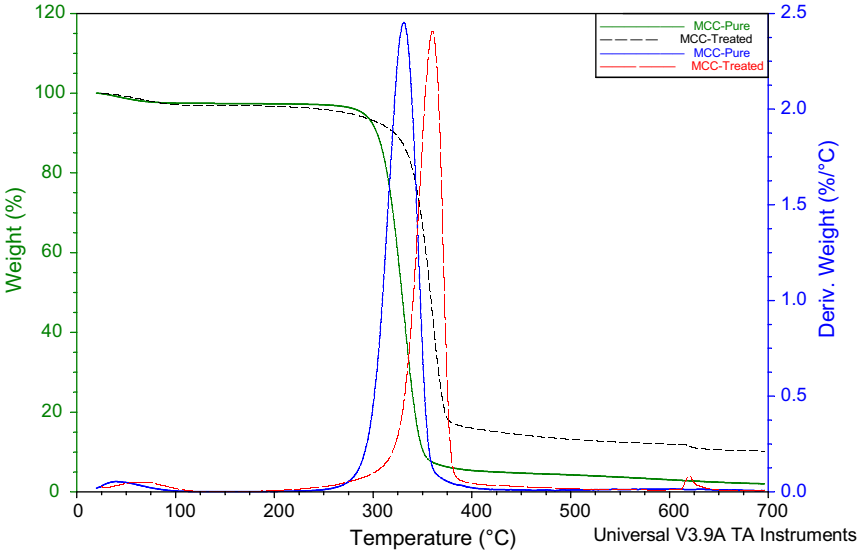

Fig. 13. TGA and DTG thermograms of unmodified and modified MCC.

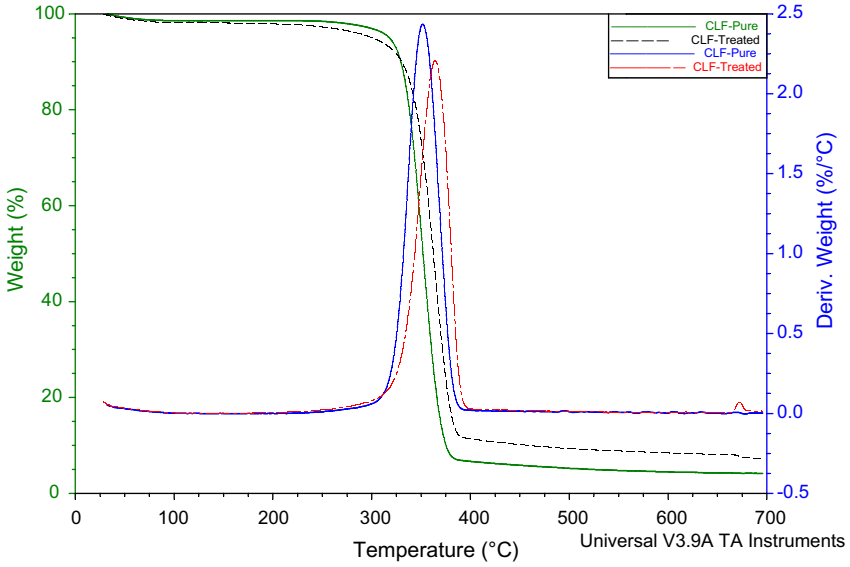

Fig. 14. TGA and DTG thermograms of unmodified and modified CLF.

the DTG thermogram (Fig. 13) shows that and the peak degradation temperature for unmodified MCC was at 330.5 °C. For Fe-modified MCC the degradation temperature range was from 339.5 to 371.5 °C and the peak degradation was at 360.3 °C. The results clearly shows that the thermal stability increased by modification of MCC with iron salts. The percentage weight of fiber residue after heating up to 700 °C was ≈8% higher for Fe-modified MCC when compared to unmodified. This implies that there was presence of iron in Fe-modified MCC which was not degraded when the samples were heated up to 700 °C. The higher percentage of residual mass in Fe-modified MCC is assumed to be from iron–cellulose complex as well as from unbounded iron. The TGA–DTG thermogram of unmodified CLF showed that degradation temperature range from 330.0 to 371.1 °C and the peak degradation was at 351.3 °C (Fig. 14). For Fe-modified CLF the degradation started at 339.9 °C and finished at 379.30 °C. The result shows that the degradation temperature was higher for CLF treated with iron salts. The percentage of residual mass was ≈4% higher for treated CLF which confirms the presence of complexed and or unbound iron in the sample. For both MCC and CLF the samples treated with iron salts showed a higher thermal stability compared to the untreated samples.

4. Conclusions

Cellulose, when treated in high pH with an oxidizing agent, can result in the oxidation of hydroxyl groups into ketones or carboxylates. These functional groups can readily form complexes with transition metals. FTIR spectroscopy and XPS suggests that complexation between modified cellulose hydroxyl and Fe ions. FTIR spectroscopy supported the formation of diketone linkages from both MCC and CLF, with Fe to result in complexation. The presence of iron changed the degradation temperature upon modification. The resulting modified samples of MCC and CLF may be used for many applications such as property enhancement in composite manufacturing, magnetographic printing and manufacture of security paper. The research

on using these cellulose samples modified with iron for manufacturing fiber oriented composite films by solvent casting the fiber–polymer matrix in a magnetic field is under investigation.

Acknowledgements

The authors thank Dr. Rana Sodhi at surface interface Ontario for the assistance with K-Alpha XPS. Financial support from Ontario center of excellence (OCE) is also gratefully acknowledged.

References

Allen, G. C., Curtis, M. T., Hooper, A. J., & Tucker, P. M. (1974). X-ray photoelectron spectroscopy of iron–oxygen systems. *Journal of Chemical Society, Dalton Transactions*, 1525.

Angles, M. N., & Dufresne, A. (2000). Plasticized starch/tunicin whiskers nanocomposites. 1. Structural analysis. *Macromolecules, 33*, 8344–8353.

Bielecki, S., & Krystynowicz, A. (2002). Bacterial cellulose. *Biopolymers Polysaccharides 1, 5*, 37–90.

Bock, B., Karsten, F., Helmut, J., Kuhr, M., & Musso, H. (1971). Bond character of beta diketone metal chelates. *Angewandte Chemie International Edition, 10*(4), 225.

Bordel, D., Putaux, J., & Heux, L. (2006). Orientation of native cellulose in an electric field. *Langmuir, 22*, 4899.

Cerchiaro, G., Carlos, A., Laudelina, M., Temperini, A., & Ferreira, A. M. (2005). Corrigendum to "Investigations of different carbohydrate anomers in copper (II) complexes with D-glucose, D-fructose and D-galactose by Raman and EPR spectroscopy". *Carbohydrate Research, 340*, 2352.

Coates, J. (2000). Interpretation of infrared spectra, a practical approach. In R. A. Meyers (Ed.), *Encyclopedia of analytical chemistry* (pp. 10815–10837). Chichester, UK: John Wiley and Sons Ltd.

Cranston, E. D., & Gray, D. G. (2006). Formation of cellulose based electrostatic layer by layer film in magnetic field. *Science and Technology of Advanced Materials, 7*, 319.

El-Saied, H., Basta, H. A., Abdel-hadi, A. K., & Hosny, W. M. (1994). Metal chelates with some cellulose derivatives. Part l. Preparation and characterization of chromium III carboxymethyl cellulose complexes. *Polymer International, 35*, 27.

Godovsky, D. Y., Varfolomeev, A. V., Efremova, G. D., Cherepanov, V. M., Kapustin, G. A., Volkov, A. V., et al. (1999). Magnetic properties of polyvinyl alcohol based composites containing iron oxide nano particles. *Advanced Materials for Optics and Electronics, 9*(3), 87.

Harcourt, R. D. (1972). "Increased – valence" formulas for the iron-ligand bonding of some ferrohaemoglobin compounds. *Biopolymers, 11*, 1551.

Hegetschweiler, K., Hausherr-Primo, L., Koppenol, W. H., Gramlich, V., Odier, L., Meyer, W., et al. (1995). A novel hexanuclear Fe^{III}-cis-inositolato complexes as a model for Fe^{III}-polyol interaction in aqueous solution. *Angewandte Chemie International Edition, 34*(20), 2242.

Hon, N. S. (1984). ESCA study of oxidized wood surfaces. *Journal of Applied Polymer Science, 29*, 2777–2784.

Hosny, W. M., Basta, A. H., & El-Saied, H. (1997). Metal chelates with some cellulose derivatives: V. Synthesis and characterization of some Fe III complexes with cellulose ethers. *Polymer International, 42*, 157.

Kennedy, J. F., Barker, S. A., & Zamir, A. (1974). Active insolubilized antibiotics based on cellulose–metal chelates. *Antimicrobial Agents and Chemotherapy, 6*, 777.

Kvien, I., & Oksman, K. (2007). Orientation of cellulose nanowhiskers in polyvinyl alcohol. *Applied Physics-A, 87*, 641.

Larenjeria, E., Carvalho, L. H., Silva, S. M., & D'Almedia, J. R. M. (2006). Influence of fiber orientation on the mechanical properties of polyester/jute composites. *Journal of Reinforced Plastic and Composites, 25*(12), 1269.

Lewin, M., & Ettinger, A. (1969). Oxidation of cellulose by hydrogen peroxide. *Cellulose Chemistry and Technology, 3*(1), 9–20.

Muller, L. L., Hebert, J. J., & Rollins, M. L. (1971). Electron microscopic investigation of cerium – cotton cellulose reactions. *Journal of Applied Polymer Science, 15*, 1425.

Nelson, M. L. (1964). Relation of certain infrared bands to cellulose crystallinity and crystal lattice type. Part 11. A new infrared ratio for estimation of crystallinity in celluloses I and II. *Journal of Applied Polymer Science, 8*, 1325–1341.

Offiong, E. O. (1995). Studies on the stereochemistry of diphenyl diketone monothiosemicarbazone and its transition metal complexes. *Transition Metal Chemistry, 20*, 126–131.

Oh, S. Y. et al. (2005). Crystalline structure analysis of cellulose treated with sodium hydroxide and carbon dioxide by means of X-ray diffraction and FTIR spectroscopy. *Carbohydrate Research, 340*, 2376–2391.

Olowe, A. A., Marie, Y., Refait, P., & Genin, M. R. (1994). Mechanism of formation of delta FeOOH in a basic aqueous medium. *Hyperfine Interactions, 93*, 1783.

Samal, R. K., Satrusallya, S. C., & Sahoo, P. K. (1984). Graft copolymerization of MMA onto cellulose. *Journal of Applied Polymer Science, 29*(1), 319.

Skopenko, V. V., Amirkhanov, V. M., Sliva, T. Y., Vasilchenko, I. S., Anpilova, E. L., & Garnovskii, A. D. (2004). Various types of metal complexes based on chelating beta-diketones and their structural analogues. *Russian Chemical Reviews, 73*(8), 737.

Spikes, G. H., Bill, E., Weyhermuller, T., & Wieghardt, K. (2008). Transition-metal complexes with singly reduced 1,2-diketone radical ligands. *Angewandte Chemie, 47*, 2973.

Sturcova, A., Davies, G. R., et al. (2005). Elastic modulus and stress transfer properties of tunicate cellulose whiskers. *Biomacromolecules, 6*, 1055–1061.

Sugiyama, J., Chanzy, H., & Maret, G. (1992). Orientation of cellulose microcrystals by strong magnetic fields. *Macromolecules, 25*, 4232.

Wijnja, H. A., & Schulthess, C. P. (2001). Carbonate adsorption mechanism on goethite studied with ATR-FTIR, DRIFT, and proton coadsorption measurements. *Soil Science Society of America Journal, 65*, 324.

Zeronian, S. H., & Inglesby, M. K. (1995). Bleaching of cellulose by hydrogen peroxide. *Cellulose, 2*, 265.